Design and experimental study of a small scale adsorption desalinator

Design and experimental study of a small scale adsorption desalinator

C. Olkis[a], S. Brandani[a] and G. Santori[a]*

[a]*The University of Edinburgh, School of Engineering, Institute for Materials and Processes, Sanderson Building, The King's Buildings, Mayfield Road, EH9 3BF Edinburgh, Scotland, UK*

*Corresponding author: G.Santori@ed.ac.uk

HIGHLIGHTS

- Design and experimental results of the world's most compact adsorption desalinator for the first time
- Achieving a Specific Daily Water Production of 7.7 $kg_w/(kg_{sg}d)$ and Performance Ratio of 0.6
- The small scale is not detrimental to the performance as the system is on a par with the best performing system in the literature
- A novel thermal response experiment informs about the partition of energy, the heat of adsorption, and water production

---

Abstract

Adsorption desalinators produce potable water from seawater using low-grade heat at 50-90 °C. The technology has been proven using several experimental systems, but their sizes are too large to allow efficient further development it by testing novel adsorption materials and components. In this study, we introduce the world's most compact adsorption desalinator with a bed size of 0.2 kg silica gel. The system achieves a Specific Daily Water Production of 7.7 kg_{water} per $kg_{silica\text{-}gel}$ and day. The performance is comparable to the best performing system to date proving that the downscaling is not detrimental. Moreover, the tests demonstrate the benefits of simple heat integration between the adsorber beds, which reduces energy consumption by 25 % and increases the Performance Ratio to 0.6. The importance of heat integration is further highlighted in an unprecedented thermal response experiment, which evaluates the partition of energy input in terms of sensible heat and heat of desorption.

Keywords:
Adsorption, desalination, silica gel, low grade heat, performance, waste heat recovery

The short version of the paper was presented at ICAE2018, Aug 22-25, Hong Kong. This paper is a substantial extension of the short version of the conference paper

1. Introduction

Two-thirds of the world population are already facing severe water scarcity for at least one month each year [1], future climate change and a growing world population can only worsen the situation. Consequently, seawater desalination has generated considerable recent research interest. Desalination can either be thermally driven or electrically in membrane processes, which consume 75.2 TWh/year of electricity [2]. One possibility to mitigate water scarcity is thermal desalination powered by waste heat, which is available in large quantities from manufacturing, transport and power plants [3, 4] as 72 % of global primary energy is emitted as waste heat [5]. Adsorption desalinators utilise low-grade heat sources down to 50 °C [6] and have one of the lowest electricity consumption among all thermal desalination systems [7]. The technology evolved from adsorption chillers [8, 9], which can use water-silica gel as well as other working pairs [10]. Adsorption chillers and desalinators are the same devices [11], but operated differently [12]. Another promising application for adsorption chillers is thermal storage [13, 14]. Moreover, an adsorption desalination system can also be connected with Multi Effect Distillation (MED) as a hybrid process [15]. Here, the adsorption system is operated as a combined chiller and desalinator, which cools the last effect of MED to 5 °C [15]. Shahzad et al. presented an increased overall efficiency of the hybrid process [15], while Thu et al. reported that hybridisation increases the distillate output of an existing MED plant [16]. Another promising application for adsorption desalination as well as other thermal desalination methods is the combination with Reverse Electrodialysis [17] to generate electricity from low-grade heat in a closed-loop system [18, 19]. Membrane distillation [20, 21], MED [22], and adsorption desalination [23] have been proposed for the application in closed-loop systems.

In recent years, researchers have built and studied experimental adsorption desalinators of different sizes and bed numbers. Single bed systems have the simplest process design, but can only be operated intermittently. Multi-bed prototypes can be operated semi-continuously and hence they are more industrially relevant. Ng et al. developed a prototype with four adsorption beds each contains 36 kg of silica gel [24, 25], they installed heat and mass recovery systems for the adsorber beds to improve the energy efficiency by 43 % [26]. Additionally, heat integration between the evaporator and condenser further improve the performance [6, 27]. This four bed prototype is the largest and best performing silica gel system tested to date with a Specific Daily Water Production (SDWP) of up to 14.2 $kg_w/(kg_{sg}d)$ using a heat source temperature of 85 °C [27] and 10 $kg_w/(kg_{sg}d)$ at 70 °C [6]. In addition, they reported a Performance Ratio of up to 0.73 [6]. Mitra et al. built a four bed silica gel desalinator, which is operated as a two bed, two stage system, but without heat integration and it has the lowest performance of less than 1 $kg_w/(kg_{sg}d)$ [28]. The first stage has a bed size of 5.6 kg packed in a heat exchanger of 25 kg and the second stage contains 3.2 kg per bed in a heat exchanger of 22 kg leading to a weight ratio of 5.34. Bendix et al. reported a metal-to-adsorbent weight ratio of 1 as the optimum [29]. The two bed desalinator presented by Alsaman et al. utilises 6.8 kg of silica gel in each bed with no heat integration [30]. A single bed adsorption desalinator was designed by Wu et al. with a bed containing 2.1 kg of silica gel [31]. Youssef et al. tested moved away from silica gel and tested commercial CPO-27(Ni) metal organic frame work in a single bed adsorption desalinator [32], where 0.67 kg of CPO-27(Ni) were packed in a heat exchanger of 29.3 kg metal mass. The

combined metal mass of all heat exchangers within their system amounts to 59.5 kg [32] and an adsorber heat exchanger to adsorbent weight ratio of 44, which is the highest reported in the literature.

The proposed prototypes are usually large with multiple beds up to 36 kg each or 144 kg in total [7], whereas the smaller systems only have one adsorber bed. The large scale has the advantage of being more industrially relevant, but to change the adsorbent, heat exchangers, or other components is more difficult and costly.

Current systems presented in the literature are well suited to test commercially available materials, but are not able to test innovative materials developed in a lab, which can only be obtained in the smallest quantities. There remains a strong need for small-scale systems to advance on the material side by testing novel, non-commercial materials on a system level.

In this study, we introduce a novel, small-scale adsorption desalinator. The system features two adsorber beds for semi-continuous operation and a heat integration system between the beds. The prototype distinguishes itself from previous systems through two novel aspects: its small scale and modular design. Compared to other systems, the bed size is reduced by two orders of magnitude to 0.2 kg of silica gel. The small scale will enable the testing of novel, non-commercial materials in the future and further develop adsorption materials. Further benefits of the small-scale are the reduction in laboratory space requirements and the utilisation of a small heat source like a standard thermostatic bath. All system components are easily interchangeable to facilitate the optimisation of the system and process. The experimental study presented compares the performance to larger systems in the literature. It is of utmost importance to the success of the scale-down to establish that the small size is not detrimental to the system performance. The impact of heat recovery on energy consumption is determined in two steps. Firstly, based on the key performance indicators such as Specific Daily Water Production and Performance Ratio. Secondly, a novel thermal response method was developed using very long pre-heating times to visualise the thermal energy input more clearly and provide more detail on the process. Three system configurations are tested: the system without adsorbent or heat recovery; with adsorbent, but without heat recovery; with adsorbent and heat recovery. Inferences are drawn from the three experiments on the peak energy inputs, an experimental Specific Energy Consumption analysis, and the partition of energy between metal mass and silica gel.

2. The prototype and process design

The adsorption desalinator is designed to utilize low-grade heat between 50-90 °C. The system consists of four vacuum vessels: two adsorbers each connected to the evaporator and condenser. Each vessel is equipped with a heat exchanger, a pressure transducer and thermocouples. Two water loops simplify the piping of the system [33] and supply water from the thermostatic baths to the heat exchangers. The thermostatic baths provide heating or cooling water at three different temperature levels: cold, ambient and hot (Fig. 1a). Much larger heat sources are usually required to supply the beds of adsorption desalinators. Regular thermostatic baths are sufficient to heat and cool the 0.2 kg of silica gel inside each bed. A heat recovery system improves the energy efficiency of the system by connecting the two adsorbers (Fig. 1a). The heat recovery allows cold water to flow through the hot bed first, where it takes up the heat

and through the cold bed to transfer heat from one bed to the other. No additional pumps are required for the heat recovery, because the pumps of the thermostatic baths are sufficient to pump water through two beds in series.

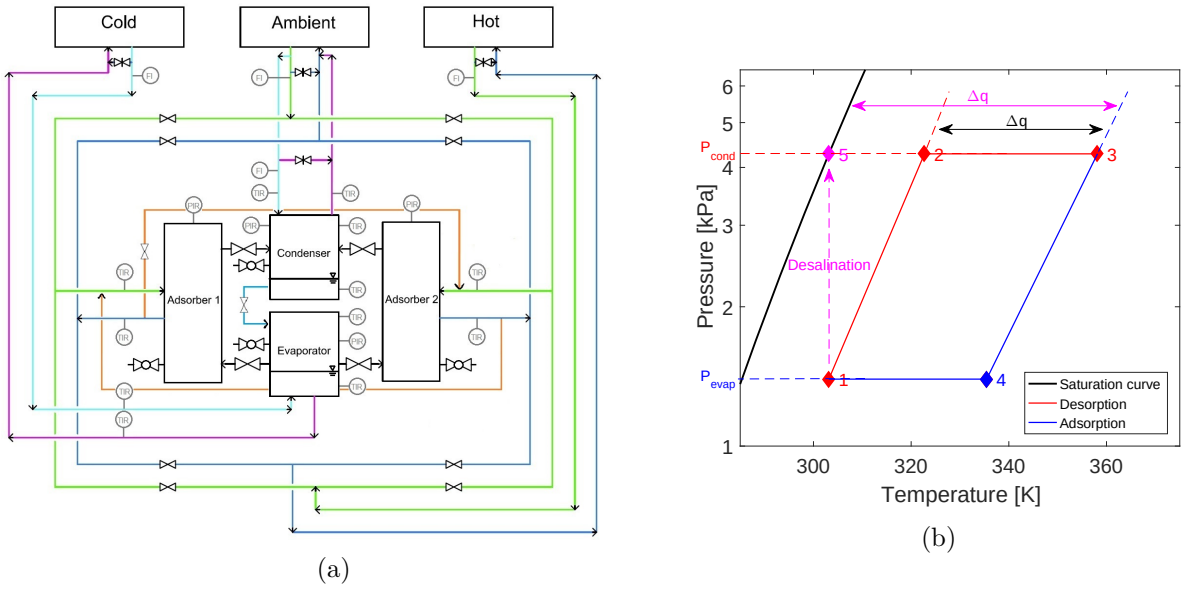

(a) (b)

Figure 1: (a) The flow diagram of the adsorption test rig including a recirculation loop between the condenser and evaporator and heat recovery connections between the adsorber beds (orange lines). The vacuum is pulled through the vacuum ball valves from each vessel.
(b) The ideal adsorption cycle for each of the beds: $1 \rightarrow 2 \rightarrow 3 \rightarrow 4 \rightarrow 1$ = Refrigeration. $5 \rightarrow 3 \rightarrow 5$ = Desalination. Δq = working capacity [g_w/g_{sg}].

Each one of the beds undergoes cyclic heating and cooling to perform the adsorption cycle shown in Fig. 1b. During the desorption step, the cold, saturated bed is heated and disconnected from the evaporator and condenser (isosteric heating). The pressure of the bed increases until it reaches the condenser pressure. The bed is then connected to the condenser and water vapour desorbs from the silica gel and condenses on the cold surface of the condenser heat exchanger. Once the bed is regenerated, the valves connecting it to the condenser and evaporator are closed and the bed is cooled to decrease the pressure again (isosteric cooling). When the pressures of the adsorber bed and evaporator are equal, the valve between the two vessels is opened. As a result, the silica gel bed adsorbs water vapour from the evaporator, which is partially filled with water. A semi-continuous mode of the test rig is ensured by regenerating one bed, while the other bed adsorbs.

A two-dimensional drawing of the test rig is shown in Fig. 2b, which illustrates the small size of the system. The height of the system is less than 500 mm, the width and length are less than 300 mm. This small-scale, modular design allows a higher flexibility in changing components, adsorption materials and fluids. The system consists of four 316L stainless steel vacuum vessels, which are the evaporator, condenser and two adsorber vessels. The leak rates of the vessels are between $5 \cdot 10^{-7}$ Pa·m^3/s and $8 \cdot 10^{-7}$ Pa·m^3/s, which means that a vacuum pump is only initially needed to pull a vacuum.
Inside each one of the vessels is an aluminium heat exchanger connected to the heating and cooling water system. All of the vessels are equipped with ISO-KF flanges and are connected

through electro-pneumatic valves (Pfeiffer Vacuum GmbH, Germany). A pressure transducer is fitted to each vessel (WIKA Alexander Wiegand SE & Co. KG, Germany, 0.25 % accuracy). Both, the evaporator and the condenser feature viewports (Pfeiffer, Germany) to check the water level and for the formation of vapour bubbles during evaporation. The evaporator and condenser are equipped with T-Type thermocouples (Omega Engineering, USA, 0.4 % accuracy), which measure the temperatures of the vapour and liquid phases. Additional thermocouples are placed at the outlet and inlet to the heat exchangers of all four vessels. These thermocouples are used to determine the temperature difference of the heating and cooling water supplied to the heat exchangers.

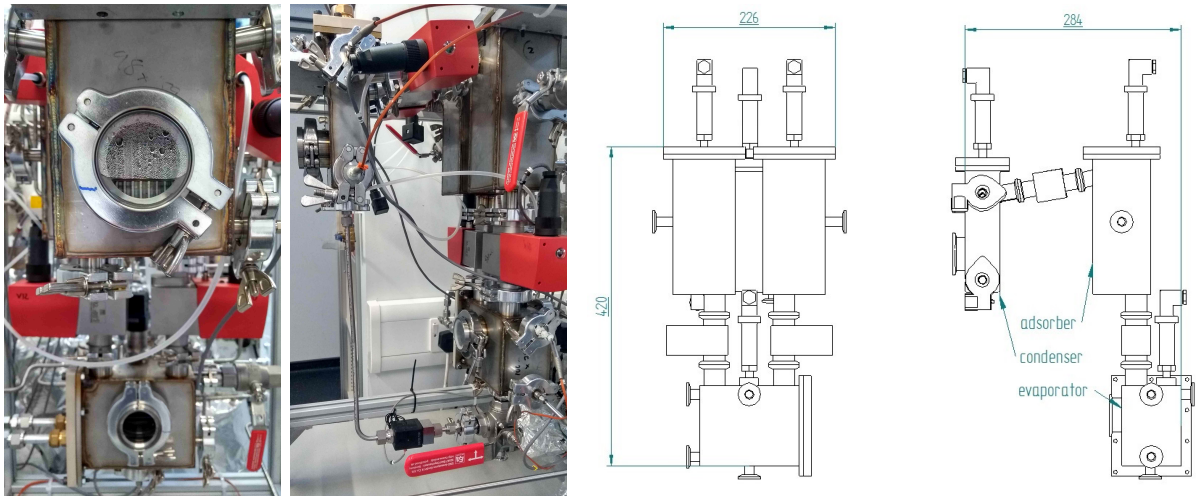

(a) (b)

Figure 2: (a) Photographs of front and side of the system
(b) A Computer-aided design drawing of the system in front and side view with dimensions [mm]

The aluminium heat exchangers inside the adsorber vessels are shown in Fig. 3a (RC Racing Radiators, Italy). The spaced between the fins of the heat exchanger are 5 mm and are filled with micro-porous silica gel beads (0.5 - 2 mm diameter, Siogel Oker-Chemie GmbH, Germany). Siogel silica gel [34, 35] is a newer adsorption material than Fuji Davison silica gel RD with similar properties [36]. The silica gel beads are secured inside the heat exchanger with a 290 µm polymer mesh (Plastok Meshes & Filtration Ltd, UK) with an open area of 50 %. The mesh is assembled to the heat exchanger by Loctite 454 instant adhesive (Henkel AG & Co. KGaA, Germany). Each heat exchanger has a weight of 600 g and is filled with 210 g of silica gel resulting in a metal-to-adsorbent weight ratio of 2.86 (Fig 3a). The aluminium heat exchangers of the evaporator and condenser are shown in Fig. 3b with a mass of 150 g and 415 g respectively. The evaporator heat exchanger is placed flat, horizontally, and fully submerged in the liquid phase, while the condenser heat exchanger is operated horizontally in the vapour phase. The finned design of the condenser heat exchanger allows condensed water droplets to flow down the heat exchanger towards the bottom of the condenser vessel.

A polyetheretherketone *PEEK* plate (RS Components Ltd., UK) is assembled to each heat exchanger by using brass fittings (Giacomini S.p.A., Italy), which prevent vacuum leakage with a fluoroelastomer O-ring. The assembly of heat exchanger, PEEK plate, pressure transducer and brass fitting is displayed in Fig. 3a. In addition, each stainless steel vessel features an

O-ring groove, where another fluoroelastomer O-ring (Polymax Ltd., UK) is pressed between the PEEK plate and the respective stainless steel vessel to assure vacuum tightness.

(a) (b)

Figure 3: (a) Photograph of the front and side of the aluminium heat exchangers packed with silica gel, which is secured by the mesh. PEEK plates, pressure transducers, and fittings are mounted on top of the heat exchangers. (b) Photograph of the aluminium heat exchangers used for evaporator (left) and condenser (right).

The overall system fits on a workbench of 2 m length and 1 m width in Fig. 4. On the left side of the bench, the frame with the adsorption test rig is placed. In the middle, the heating and cooling water pipes are located along with rotameters (Nixon Flowmeters, UK, 1.6 % accuracy), which are required to set the water flow rate to each of the heat exchangers. The heating and cooling water cycle system is connected to the thermostatic baths (Julabo GmbH, Germany), which is an advantageous feature of the system. Usually the energy requirements of adsorption desalinators are vast and exceed the heating/cooling capacity of a thermostatic bath by far. Furthermore, the internal pumps of the thermostatic baths are sufficient to supply water to the heating/cooling cycle.

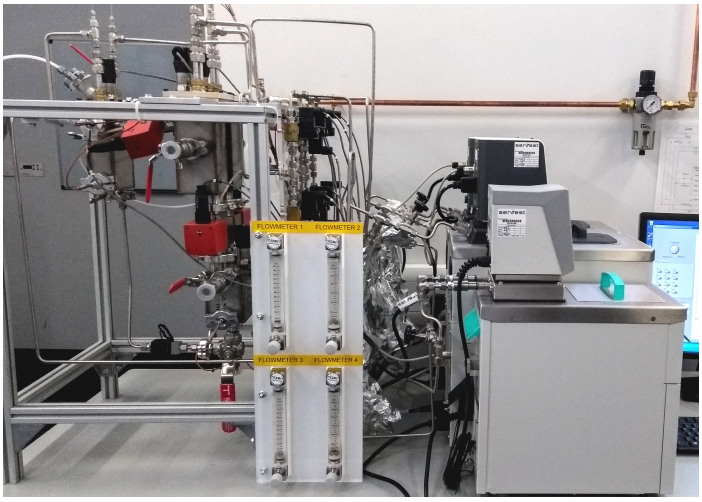

Figure 4: Side view of the work bench with the adsorption test rig on the left, the heating/cooling pipework in the centre, and the thermostatic baths on the right.

The pressure and temperature sensors are directly connected to a data acquisition and control

board (Advantech Co. Ltd., USA). The sensors are monitored using a PC by a control code based on LabVIEW software (National Instruments Corp., USA). The Labview code was specifically designed and customised for the test rig. The code allows the adjustment of cycle times, actuates the valves, and saves all the data from the sensors to a text file. The thermostatic bath temperatures and flow-rates are set manually and are kept constant throughout an experiment.

3. Experimental analysis

Fig. 5a shows the temperatures measured at the outlets of each heat exchanger during an exemplary experimental run of the test rig. It can be seen that the two adsorber beds undergo cyclic heating and cooling, where the hot bed desorbs water vapour to the condenser, while the cold bed adsorbs water vapour from the evaporator. Evaporator and condenser remain at constant temperature and pressure. Different temperatures in each vessel can be adjusted through the thermostatic baths, which has a significant impact on the system performance and the water uptake of the adsorption material. Another important system parameter is the cycle time as there is a trade-off between cycle frequency and water uptake. The water uptake increases over time until saturation, while the rate of adsorption decreases over time. In addition, faster cycles increase the energy consumption as the metal of the heat exchangers has to be heated and cooled during each cycle. The temperature readings can be used to calculate the water production $\dot{m}_w$ inside the condenser in Fig 5b.

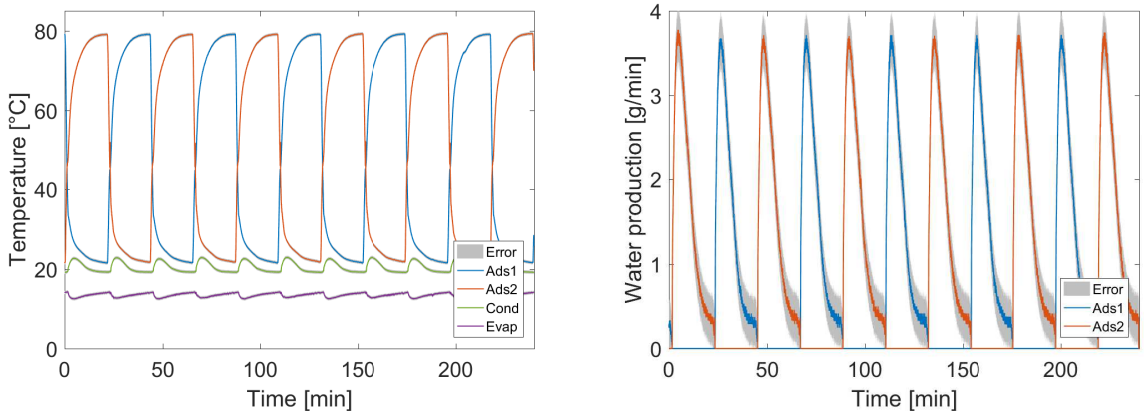

(a) (b)

Figure 5: (a) The temperature curves measured at the heat exchanger outlets of each vessel during an experiment at $T_{hot,in}$ = 80 °C, $T_{cond,in}$ = 20 °C and $T_{evap,in}$ = 15 °C with a half cycle time of 1200 s.
(b) The corresponding water production from the same experiment.

Heat losses have been neglected, because the evaporator and condenser both operate at ambient temperature in adsorption desalination, therefore with negligible heat losses. The adsorber heat exchangers operate above ambient temperature during desorption. However, they are in a vacuum vessel, where the vacuum insulates the heat exchangers from the vessel walls. Moreover, the inlet and outlet tubes are thermally decoupled from the vessel by the PEEK plates, which further reduces heat losses.

The water production $\dot{m}_w$ is determined through an energy balance for the condenser:

$$\dot{m}_w = \frac{\dot{m}_{cond,in}\ c_{p,w}\ (T_{cond,in} - T_{cond,out})}{L} \tag{1}$$

where $\dot{m}_{cond,in}$ [kg/s] is the mass flow of cooling water supplied to the condenser heat exchanger, $c_{p,w}$ [kJ/(kgK)] is the specific heat of water, L [kJ/kg] is the latent heat, and $T_{cond,in/out}$ [K] the temperature differences between the inlet and outlet of the heat exchangers. The heat input to the desorber $\dot{Q}_{des}$ [kJ/s] is calculated using the following equation:

$$\dot{Q}_{des} = \dot{m}_{des,in}\ c_{p,w}\ (T_{des,in} - T_{des,out}) \tag{2}$$

where $\dot{m}_{des,in}$ represents the inlet flow rate of heating water to the adsorption bed [kg/s] and is required to determine the dimensionless Performance Ratio PR [-]:

$$PR = \int_0^{t_{cycle}} \frac{\dot{m}_w\ 2326\frac{kJ}{kg}}{\dot{Q}_{des}} dt \tag{3}$$

which is one of the two key performance indicators in adsorption desalination. The PR represents the water produced within the time of one cycle t_{cycle} [s] multiplied with a standardised latent heat [kJ/kg] in relation to the heat input. The PR has some limitations, because it does not take different heat source temperatures into account and it is inapplicable to membrane processes. However, it is a useful tool for the comparison of different systems of the same thermal desalination technology between each other. The second key performance indicator is the Specific Daily Water Production $SDWP$ [$kg_w/(kg_{sg}d)$] for the number of cycles performed within a day N [-]:

$$SDWP = N \int_0^{t_{cycle}} \frac{\dot{m}_w}{M_{sg}} dt \tag{4}$$

The experimental investigation can be supplemented by the Specific Energy Consumption SEC [37], which is a theoretical, thermodynamic performance indicator assessed through the thermodynamic adsorption cycle in Fig. 1b. The SEC depicts the specific energy required to heat the adsorption material and to desorb water from the material by overcoming the heat of desorption Δh [kJ/kg_w] given in [36].

$$SEC = \frac{(q_1 c_{p,w} + c_{p,sg})(T_2 - T_1) + \left[c_{p,sg} + \frac{q_2+q_3}{2} c_{p,w}\right](T_3 - T_2) + \Delta q \cdot \Delta h}{\Delta q} \tag{5}$$

3.1. Comparison with literature

The SDWP is the key performance indicator in adsorption desalination as it describes the efficiency of the adsorption material and system. The SDWP can be maximised by fast cycle times in combination with a large working capacity, which is a result of little heat and mass transfer limitations, well designed heat exchangers, and a minimised void volume within the system. In addition, the SDWP is very sensitive to the system operating parameters and is largest in desalination when evaporator and condenser operate at the same pressure as this maximises the working capacity. Cooling requires a low evaporator temperature and pressure, which reduces the working capacity of the adsorption material.

Silica gel is an inexpensive, commercially available adsorption material. Thus, silica gel is commonly used as benchmark material in adsorption desalination and it is ideal for the comparison of different system designs.

Ng et al. [7] have reported the performance of their system in several configurations, where they have achieved the best results for silica gel. The best performance was achieved with the four beds configuration and heat integration between condenser and evaporator. The heat integration lifts the evaporator inlet temperature above the condenser inlet temperature, which leads to $P_{evap} \approx P_{cond}$ as shown in Fig. 1b and improves the working capacity. In this configuration their large scale prototype with 144 kg of silica gel achieved a SDWP = 14.2 $kg_w/(kg_{sg}d)$ at $T_{hot,in}$ = 85 °C. The experiments of the four bed system [6, 27] were not compared to the two bed system presented here.

Ng et al. also reported the performance of the four bed system operated in two bed mode and without heat integration between their evaporator and condenser [7]. In this configuration, their prototype achieved SDWP = 8.2 $kg_w/(kg_{sg}d)$ at $T_{hot,in}$ = 80 °C, $T_{evap,in}$ = $T_{cond,in}$ = 30 °C, and a half cycle time of 600 s as displayed in Fig. 6 for comparison. At the same conditions, the adsorption desalinator introduced in this study reached SDWP = 7.7 $kg_w/(kg_{sg}d)$, which is 6 % lower. All other desalinators reported in the literature and utilising silica gel have much lower performances [28, 30]. Ng et al. have proposed the largest system with a total of 72 kg of silica gel in two beds mode, while the desalinator of this study is the smallest system design with a total of only 0.4 kg of silica gel. Hence, the smallest and the largest systems achieve the best performances in the literature highlighting that for properly designed systems the system size is irrelevant to the performance.

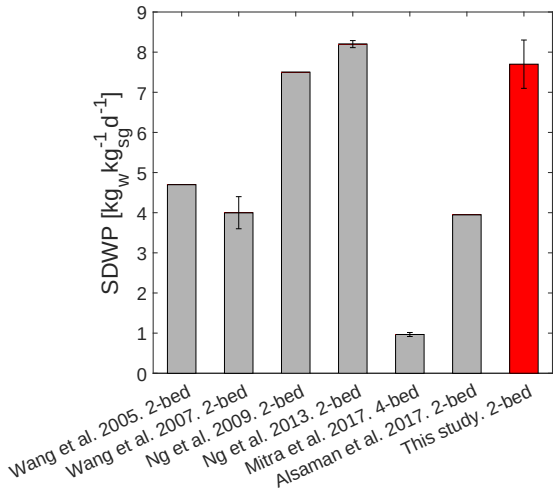

Figure 6: The systems performance in comparison to the best experimental results reported in the literature for silica gel [7, 26, 28, 30, 38, 39]. The highest SDWP in this study was achieved at $T_{evap,in}$ = $T_{cond,in}$ = 30 °C, $T_{hot,in}$ = 80 °C and a half cycle time of 600 s.

The following considerations extend the scope of SDWP ≈ 8 $kg_w/(kg_{sg}d)$ in Fig. 6 to a potential application of an adsorption desalinator for residential households, e.g. an average household in southern Italy consumes about 400 kg of water per day [40]. Thus, the adsorption material required per household is $400\frac{kg_w}{d}$ / $8\frac{kg_w}{kg_{sg}d}$ = 50 kg_{sg}. Advances in novel adsorbents [41] could reduce this number to 20 kg of adsorption material per household. An adsorption desalinator

with 1 ton of material can already supply 20 households today or 50 in the future. Therefore, adsorption desalination plants are well suited for smaller applications, e.g. providing smaller seaside communities in dry regions with drinking water. For small applications, the technology even offers an alternative to reverse osmosis as it can be powered by solar collectors [30] and requires a minimum of maintenance compared to membrane processes [7, 42].

3.2. Impact of heat recovery

The first set of experiments were conducted with the basic system set-up without heat recovery or recirculation line. The PR without heat integration was 0.48 at long cycles times as shown in Fig. 7a. The heat recovery has the largest impact on the PR at very short half cycle times, where it improves the PR by a factor of three from 0.10 to 0.33 at 200 s. This half cycle time leads to a high frequency of heating and cooling the adsorber beds. The working capacity of the silica gel is reduced at short cycle times, while the aluminium heat exchangers have to be heated and cooled from ambient temperature to 80 °C during each cycle regardless of the cycle time requiring a fixed amount of energy to heat the metal mass Q_{alu}. At short cycle, times the material adsorbs little water during each cycle, while the metal mass needs to be heated and cooled at high frequency leading to a low PR. At long cycle times the working capacity of the material increases towards equilibrium, while the impact of Q_{alu} on the PR becomes less dominant. Therefore, the impact of the heat recovery on the PR decreases, but the PR remains 25 % higher even at long cycle times with a maximum PR of 0.6.

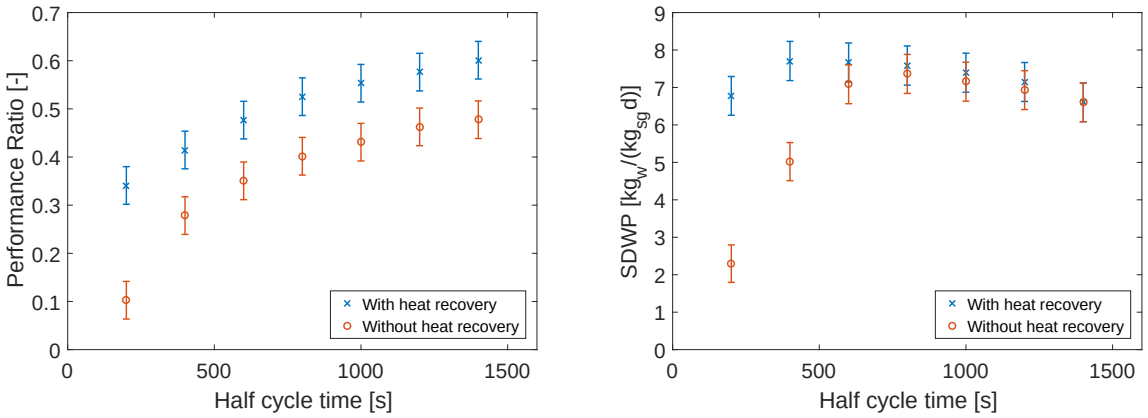

(a) (b)

Figure 7: (a) The impact of the heat recovery on the Performance Ratio for varying cycles times at $T_{evap,in} = T_{cond,in} = 30$ °C, $T_{hot,in} = 80$ °C.
(b) The comparison of the Specific Daily Water Production with and without heat recovery under the same conditions as in (a).

At half cycle times longer than 600 s the SDWP is essentially independent of the heat recovery (Fig. 7b). By contrast, the heat recovery has a large impact on the SDWP at half cycle times below 600 s, which is unexpected as the SDWP in eq. (4) is independent of the heat input to the adsorbers. The heat recovery reduces the external heat input into the adsorbers, but does not affect the condenser. Thus, the impact of heat recovery should improve the PR, but not the SDWP. The sharp drop in PR and SDWP below 400 s can be explained by looking at the condenser inlet temperature. The inlet temperature is set to 30 °C in all cases of Fig. 7 and

the thermostatic baths can provide this inlet temperature except for two cases: 200 s and 400 s without heat recovery. Here, the frequency of the cycles and heat input are too high for the bath to cool the returning ambient water to the set temperature leading to $T_{cond,in}$ = 36 °C instead of 30 °C, which reduces the working capacity. The heat recovery overcomes this system limitation by reducing the peak energy input. Therefore, less cooling power needs to be provided and the overall system can cope with the fast cycles in virtue of the heat recovery system.

Wang et al. [26] investigated the impact of heat recovery on their two bed adsorption system for full cycle times of 250 s to 600 s with T_{hot} = 85 °C, T_{cond} = 29.4 °C, and T_{evap} = 12 °C. They reported an improvement of the PR by 30 % at short cycle times and 16 % at long cycle times on a two beds adsorption system. Hence, their results are comparable to this study with the exception of the very short half cycles in Fig. 7a. In addition, they implemented a mass recovery step equilibrating the pressure of the two adsorber beds by opening a valve between them, when switching the cycle from adsorption to desorption. Implementation of mass recovery in combination with heat recovery increased the PR of their system by 43 %.

Mass recovery is most effective at large pressure differences between evaporator and condenser as it is the case in their study [26]. The large pressure difference between P_{evap} and P_{cond} is present in cooling applications, where the mass recovery shortens the isosteric cooling time and increases the working capacity. However, in desalination applications mass recovery is not beneficial, because the evaporator and condenser operate at $P_{evap} \approx P_{cond}$ leading to one constant pressure throughout the entire system. Therefore, opening a valve between the two beds at the end of a cycle does not lead to any vapour flow, because no pressure gradient is present within the system. As a result, the performance of an adsorption desalinator cannot be significantly improved with a mass recovery.

3.3. Characterisation of the adsorber

The performance ratio indicates the energy efficiency, but does not provide information on how the energy input is used in the system. The energy input during desorption contributes to heating of the aluminium heat exchangers, the adsorption material as well as the heat of desorption. The experimental procedure was altered to assess the energy required for each part of the process. In normal operation, the beds with the silica gel are pre-heated for less than a minute to an intermediate temperature, which increases the bed pressure. Afterwards, the adsorber is connected to the condenser and vapour desorbs from the material, while the bed is further heated up to the regeneration temperature.

The results of the experiments shown in Fig. 8 allow to separate the energy required to heat the beds from the heat of desorption. At first, the energy input of the blank heat exchanger without silica gel was measured by cycling the empty heat exchanger in temperature swings. This first step determines the sensible heat of the metal mass of the heat exchanger. Afterwards, the beds were packed with silica gel to repeat the temperature swings, but the preheating time was extended from 1 min to 20 min as opposed to a normal experiment. During the pre-heating phase, the beds are completely heated up to the regeneration temperature, while only limited desorption takes place. Hence, almost all the energy input can be associated with heating the aluminium heat exchangers and the silica gel beads. After 20 min of pre-heating, the valve between the adsorber and condenser is opened to desorb water for another 20 min. Moreover,

on the basis of the blank experiment it is possible to quantify the sensible heat of the metal mass and the sensible heat of the silica gel. These experiments allow the sensible heat of the metal mass and silica gel to be separated from the heat of desorption.

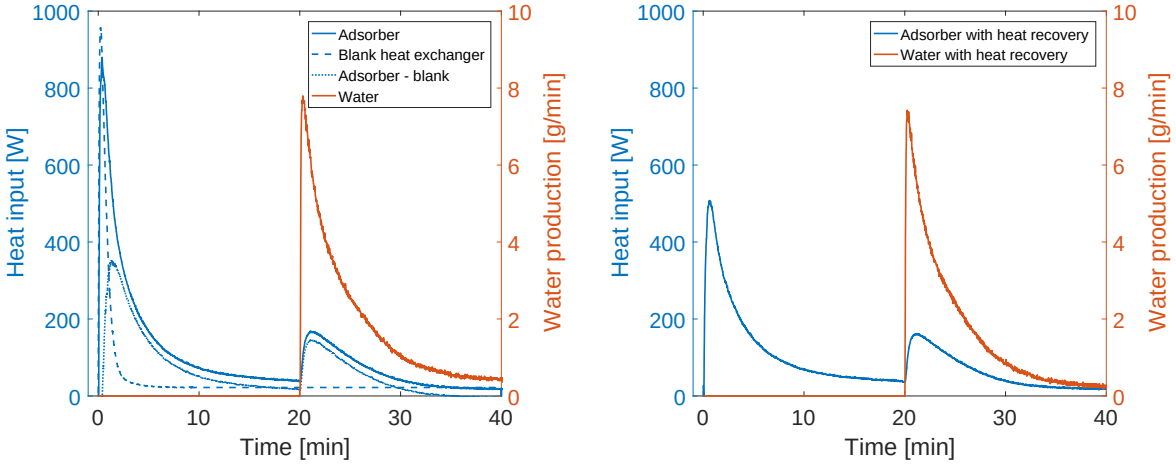

Figure 8: The energy input to the adsorber beds and water production at 20 min of pre-heating and 20 min of desorption:
(a) Without heat recovery: Two different experiments, where the empty, blank heat exchangers and the heat exchangers packed with silica gel were tested. In addition, the difference between the two is plotted to illustrate the energy required by the silica gel alone neglecting the heat exchanger itself.
(b) With heat recovery: The energy input and water production with heat recovery of the adsorber bed packed with silica gel and tested in a third experiment.

The peak of the heat input between t = 0-5 min in Fig. 8 can be attributed to heating the heat exchangers, silica gel and the adsorbed water from ambient temperature up to the regeneration temperature. Here, the experiment with the blank heat exchanger without silica gel shows the highest and shortest peak. This experiment depicts the energy required to heat the aluminium alone that comes to (103 ± 5) kJ, which is 40 % of the entire energy input to the system.
The result of the blank experiment was subtracted from the original experiment of the heat exchanger containing material. The resulting curve of the difference shown in Fig. 8a represents the energy input ascribed to the silica gel alone neglecting the aluminium heat exchanger (sg alone). The energy required to heat the silica gel amounts to (153 ± 21) kJ and includes the sensible heat of the silica gel and partial water desorption. Some of the adsorbed water desorbs during the pre-heating phase, because the extensive heating to the regeneration temperature causes the material to leave the isostere. The partial desorption can be derived from the second peak of the heat input, which represents the heat of desorption.
A total of (40.6 ± 0.6) g of water was produced during desorption shown in Fig. 8a between 20 to 40 min. The ratio of the heat input of the second peak to the amount of desorbed water is (1850 ± 100) kJ/kg_w and can be ascribed to the heat of desorption. However, the heat of desorption is always greater than the latent heat L(25 °C) = 2441 kJ/kg_w [43]. Therefore, a part of the water desorbs during the long pre-heating phase with water vapour filling the void volume in the adsorbers. The ratio of the energy input without the aluminium heat exchanger to the produced water results in the Specific Energy Consumption leading to an experimental SEC_{exp} = (3770 ± 520) kJ/kg_w. In comparison, the thermodynamic SEC calculated with

eq. (5) predicts SEC = 3400 kJ/kg_w. Thus, SEC_{exp} deviates by 10 % from the thermodynamic SEC. The small deviation is due to the very long half cycle time of 40 min reducing heat and mass transfer limitations significantly.

A third experiment was conducted to assess the energy savings using heat recovery (Fig. 8b). The energy input with heat recovery amounts to (216 ± 18) kJ, which is 16 % less than the energy input without heat recovery. The energy savings of 16 % confirm the results of the PR analysis in Fig. 7a. Water production is not effected by heat recovery, which is why the reduction of the energy input by 16 % also reduces the PR. In addition, the peak power input is almost halved from 850 W to 500 W due to heat recovery. Hence, heat recovery allows the system to be connected to a smaller heat source to meet peak demand.

4. Conclusion

A novel, small-scale adsorption desalination prototype was designed, assembled and is introduced here. The test rig is currently the world's smallest design. The small-scale design allows an increased flexibility in testing new materials and system components compared to larger system designs. The first part of the experimental investigation assessed the performance of Siogel silica gel packed inside the aluminium heat exchangers. This starting point established a reference case, which is compared to the literature. The system achieved a Specific Daily Water Production of up to 7.7 $kg_w/(kg_{sg}d)$, which is among the highest results reported for silica gel. Hence, the small scale is not detrimental to the performance and a full analysis of novel adsorption materials is possible with this small-scale system in the future. Moreover, the impact of heat recovery between the adsorber beds on the system performance was investigated in two steps by focusing on the performance indicators and by a thermal response experiment. The performance ratio was increased by 25 % to 0.6 by the application of heat recovery, while the thermal response experiment gave compelling insight into the adsorption process with and without heat recovery. The thermal response analysis showed that heating the metal mass of the system requires 40 % of the entire energy input to the system. The experimental Specific Energy Consumption of the silica gel material amounts to 3770 kJ per kg of water, which deviates from the theoretical value by 10 %. Heat recovery halves the peak heat demand allowing a more stable process.

Acknowledgements

The authors are grateful to Dr. Rhys Lloyd for his support during the preparation of the manuscript. This work was performed within the RED-Heat-to-Power project (Conversion of Low-grade Heat to Power through closed loop Reverse Electro-Dialysis) - Horizon 2020 programme, Project Number: 640667: `www.red-heat-to-power.eu`

Nomenclature

General

$c_{p,w}$	Specific heat water (kJ/(kgK))
L	Latent heat (kJ/kg$_w$)
M_{sg}	Mass of silica gel (kg$_{sg}$)
N	Number of cycles per day (-)
P	Pressure (kPa)
Q	Heat (kJ)
q	Adsorption uptake (g$_w$/g$_{sg}$)
T	Temperature (K)
t_{cycle}	Cycle time (s)
Δh	Heat of desorption (kJ/kg$_w$)
Δq	Working capacity (g$_w$/g$_{sg}$)
$\dot{m}_w$	Water production (kg/s)
$\dot{Q}$	Heat flow (kJ/s)

Subscripts

ads	Adsorber
alu	Aluminium
$cond$	Condenser
des	Desorber
$evap$	Evaporator
hot	Heat source
in	Inlet
out	Outlet
sg	Silica gel
w	Water

Acronyms

AD	Adsorption desalination
HR	Heat recovery
MED	Multi effect distillation
$PEEK$	Polyether ether ketone
PR	Performance Ratio (-)
$SDWP$	Specific Daily Water Production (kg$_w$/(kg$_{sg}$d))
SEC	Specific Energy Consumption (kJ/kg$_w$)

References

[1] Mesfin M Mekonnen and Arjen Y Hoekstra. Four billion people facing severe water scarcity. *Science advances*, 2(2):e1500323, 2016.

[2] Muhammad Wakil Shahzad, Muhammad Burhan, Li Ang, and Kim Choon Ng. Energy-water-environment nexus underpinning future desalination sustainability. *Desalination*, 413:52 – 64, 2017.

[3] Alexander S. Rattner and Srinivas Garimella. Energy harvesting, reuse and upgrade to reduce primary energy usage in the usa. *Energy*, 36(10):6172 – 6183, 2011.

[4] Michael Papapetrou, George Kosmadakis, Andrea Cipollina, Umberto La Commare, and Giorgio Micale. Industrial waste heat: Estimation of the technically available resource in the eu per industrial sector, temperature level and country. *Applied Thermal Engineering*, 138:207 – 216, 2018.

[5] Clemens Forman, Ibrahim Kolawole Muritala, Robert Pardemann, and Bernd Meyer. Estimating the global waste heat potential. *Renewable and Sustainable Energy Reviews*, 57:1568–1579, 2016.

[6] Kyaw Thu, Hideharu Yanagi, Bidyut Baran Saha, and Kim Choon Ng. Performance investigation on a 4-bed adsorption desalination cycle with internal heat recovery scheme. *Desalination*, 402:88 – 96, 2017.

[7] Kim Choon Ng, Kyaw Thu, Youngdeuk Kim, Anutosh Chakraborty, and Gary Amy. Adsorption desalination: An emerging low-cost thermal desalination method. *Desalination*, 308:161 – 179, 2013. New Directions in Desalination.

[8] Giulio Santori, Salvatore Santamaria, Alessio Sapienza, Stefano Brandani, and Angelo Freni. A stand-alone solar adsorption refrigerator for humanitarian aid. *Solar Energy*, 100(Supplement C):172 – 178, 2014.

[9] Alessio Sapienza, Giuseppe Gullì, Luigi Calabrese, Valeria Palomba, Andrea Frazzica, Vincenza Brancato, Davide La Rosa, Salvatore Vasta, Angelo Freni, Lucio Bonaccorsi, and Gaetano Cacciola. An innovative adsorptive chiller prototype based on 3 hybrid coated/granular adsorbers. *Applied Energy*, 179:929 – 938, 2016.

[10] Giulio Santori and Chiara Di Santis. Optimal fluids for adsorptive cooling and heating. *Sustainable Materials and Technologies*, 12:52 – 61, 2017.

[11] A. Frazzica, V. Palomba, B. Dawoud, G. Gullì, V. Brancato, A. Sapienza, S. Vasta, A. Freni, F. Costa, and G. Restuccia. Design, realization and testing of an adsorption refrigerator based on activated carbon/ethanol working pair. *Applied Energy*, 174:15 – 24, 2016.

[12] Alessio Sapienza, Valeria Palomba, Giuseppe Gullì, Andrea Frazzica, and Salvatore Vasta. A new management strategy based on the reallocation of ads-/desorption times: Experimental operation of a full-scale 3 beds adsorption chiller. *Applied Energy*, 205:1081 – 1090, 2017.

[13] Matthias S. Treier, Gunther Munz, Andreas Velte, Stefan K. Henninger, and Ferdinand P. Schmidt. Estimations of energy density and storage efficiency for cascading adsorption heat storage concepts. *International Journal of Refrigeration*, 2018.

[14] Valeria Palomba, Vincenza Brancato, and Andrea Frazzica. Experimental investigation of a latent heat storage for solar cooling applications. *Applied Energy*, 199:347 – 358, 2017.

[15] Muhammad Wakil Shahzad, Kyaw Thu, Yong deuk Kim, and Kim Choon Ng. An experimental investigation on medad hybrid desalination cycle. *Applied Energy*, 148:273 – 281, 2015.

[16] Kyaw Thu, Young-Deuk Kim, Gary Amy, Won Gee Chun, and Kim Choon Ng. A hybrid multi-effect distillation and adsorption cycle. *Applied Energy*, 104:810 – 821, 2013.

[17] F. Giacalone, C. Olkis, G. Santori, A. Cipollina, S. Brandani, and G. Micale. Novel solutions for closed-loop reverse electrodialysis: thermodynamic characterisation and perspective analysis. *Energy*, 2018.

[18] A. Tamburini, M. Tedesco, A. Cipollina, G. Micale, M. Ciofalo, M. Papapetrou, W. Van Baak, and A. Piacentino. Reverse electrodialysis heat engine for sustainable power production. *Applied Energy*, 206(Supplement C):1334 – 1353, 2017.

[19] M. Bevacqua, A. Tamburini, M. Papapetrou, A. Cipollina, G. Micale, and A. Piacentino. Reverse electrodialysis with nh4hco3-water systems for heat-to-power conversion. *Energy*, 137:1293 – 1307, 2017.

[20] G. Zaragoza, A. Ruiz-Aguirre, and E. Guillén-Burrieza. Efficiency in the use of solar thermal energy of small membrane desalination systems for decentralized water production. *Applied Energy*, 130:491 – 499, 2014.

[21] M. Micari, A. Cipollina, F. Giacalone, G. Kosmadakis, M. Papapetrou, G. Zaragoza, G. Micale, and A. Tamburini. Towards the first proof of the concept of a reverse electrodialysis - membrane distillation heat engine. *Desalination*, 453:77 – 88, 2019.

[22] George Kosmadakis, Michael Papapetrou, Bartolomé Ortega-Delgado, Andrea Cipollina, and Diego-César Alarcón-Padilla. Correlations for estimating the specific capital cost of multi-effect distillation plants considering the main design trends and operating conditions. *Desalination*, 447:74 – 83, 2018.

[23] C. Olkis, G. Santori, and S. Brandani. An adsorption reverse electrodialysis system for the generation of electricity from low-grade heat. *Applied Energy*, 231:222 – 234, 2018.

[24] KC Ng, HT Chu, and X Wang. Prototype testing of a novel four-bed regenerative silica gel-water adsorption chiller. In *International Congress of Refrigeration*, pages 0–0, 2003.

[25] Xiaolin Wang and Kim Choon Ng. Experimental investigation of an adsorption desalination plant using low-temperature waste heat. *Applied Thermal Engineering*, 25(17):2780–2789, 2005.

[26] Xiaolin Wang, Kim Choon Ng, Anutosh Chakarborty, and Bidyut Baran Saha. How heat and mass recovery strategies impact the performance of adsorption desalination plant: Theory and experiments. *Heat Transfer Engineering*, 28(2):147–153, 2007.

[27] Kyaw Thu, Bidyut Baran Saha, Anutosh Chakraborty, Won Gee Chun, and Kim Choon Ng. Study on an advanced adsorption desalination cycle with evaporator–condenser heat recovery circuit. *International Journal of heat and mass transfer*, 54(1):43–51, 2011.

[28] Sourav Mitra, Kyaw Thu, Bidyut Baran Saha, and Pradip Dutta. Performance evaluation and determination of minimum desorption temperature of a two-stage air cooled silica gel/water adsorption system. *Applied Energy*, 206:507 – 518, 2017.

[29] Phillip Bendix, Gerrit Füldner, Marc Möllers, Harry Kummer, Lena Schnabel, Stefan Henninger, and Hans-Martin Henning. Optimization of power density and metal-to-adsorbent weight ratio in coated adsorbers for adsorptive heat transformation applications. *Applied Thermal Engineering*, 124:83 – 90, 2017.

[30] Ahmed S. Alsaman, Ahmed A. Askalany, K. Harby, and Mahmoud S. Ahmed. Performance evaluation of a solar-driven adsorption desalination-cooling system. *Energy*, 128:196 – 207, 2017.

[31] Jun W Wu, Mark J Biggs, Philip Pendleton, Alexander Badalyan, and Eric J Hu. Experimental implementation and validation of thermodynamic cycles of adsorption-based desalination. *Applied Energy*, 98:190–197, 2012.

[32] Peter G. Youssef, Hassan Dakkama, Saad M. Mahmoud, and Raya K. AL-Dadah. Experimental investigation of adsorption water desalination/cooling system using cpo-27ni mof. *Desalination*, 404:192 – 199, 2017.

[33] Giulio Santori, Alessio Sapienza, and Angelo Freni. A dynamic multi-level model for adsorptive solar cooling. *Renewable Energy*, 43(Supplement C):301 – 312, 2012.

[34] G. Santori, A. Frazzica, A. Freni, M. Galieni, L. Bonaccorsi, F. Polonara, and G. Restuccia. Optimization and testing on an adsorption dishwasher. *Energy*, 50:170 – 176, 2013.

[35] Yuri I. Aristov. Adsorptive transformation and storage of renewable heat: Review of current trends in adsorption dynamics. *Renewable Energy*, 110:105 – 114, 2017. Increasing the renewable share for heating and cooling by the means of sorption heat pumps and chillers.

[36] Alessio Sapienza, Andreas Velte, Ilya Girnik, Andrea Frazzica, Gerrit Füldner, Lena Schnabel, and Yuri Aristov. "water - silica siogel" working pair for adsorption chillers: Adsorption equilibrium and dynamics. *Renewable Energy*, 110(Supplement C):40 – 46, 2017.

[37] Jun W Wu, Eric J Hu, and Mark J Biggs. Thermodynamic cycles of adsorption desalination system. *Applied Energy*, 90(1):316–322, 2012.

[38] Kim Choon Ng, Kyaw Thu, Anutosh Chakraborty, Bidyut Baran Saha, and Won Gee Chun. Solar-assisted dual-effect adsorption cycle for the production of cooling effect and potable water. *International Journal of Low-Carbon Technologies*, 4(2):61–67, 2009.

[39] Xiaolin Wang and Kim Choon Ng. Experimental investigation of an adsorption desalination plant using low-temperature waste heat. *Applied Thermal Engineering*, 25(17):2780 – 2789, 2005.

[40] Italian National Institute of Statistics (Istat). Italy in figures. Technical report, 2015.

[41] Ahmed A. Askalany, Angelo Freni, and Giulio Santori. Supported ionic liquid water sorbent for high throughput desalination and drying. *Desalination*, 452:258 – 264, 2019.

[42] Thomas Melin and Robert Rautenbach. *Membranverfahren : Grundlagen der Modul- und Anlagenauslegung*. Springer Berlin Heidelberg, 3., aktualisierte und erweiterte auflage edition, 2007.

[43] VDI-Gesellschaft Verfahrenstechnik und Chemieingenieurwesen (VDI-GVC). Wärmeatlas, vdi 10. auflage, 2006.